# Induced seismicity monitoring—comparison of surface deployed DAS arrays versus other common seismicity monitoring techniques

K. Galybin[1], M. Branston[1], M. Lal Khaitan[1]
1 SLB

## Introduction

Distributed acoustic sensing (DAS) is an established downhole logging technique in the resource industry, initially enabling acquisition of vertical seismic profiles (VSPs) (Hartog et al. 2013) and now also microseismic data (Mizuno and Le Calvez 2023). In recent years, advances in processing technology have opened the path to using horizontally deployed DAS for seismic imaging using both reflected and refracted energy (Branston et al., 2024). And now, with the proliferation of carbon capture technology, surface DAS (S-DAS) surveys have become the focus of reservoir monitoring through time-lapse seismic imaging (Yamada et al. 2024; Nakayama et al. 2025). S-DAS has been recognized as an affordable seismic sensor for reservoir monitoring. Nevertheless, monitoring objectives extend beyond seismic imaging, and detection of induced seismicity, due to injection, is an integral part of injection monitoring. This paper compares several DAS deployment scenarios: downhole, surface, and hybrid, and contrasts the performance of such networks versus conventional geophone networks, both downhole and surface.

## Microseismic Network Modelling

A 3D synthetic dynamic model was built, analogous to a Southern North Sea carbon storage location (Harrington et al. 2024), and a set of velocity and density measurements were extracted at a proposed injection site location. The data are smoothed using a 15 m Backus averaging and blocked using a 15 m minimum layer thickness criterion. The 1D model (Figure 1) is used to investigate the detectability and uncertainty of microseismic event detection at such a site using Netmod, a hydraulic fracture monitoring survey design algorithm developed by Raymer and Leslie (2011).

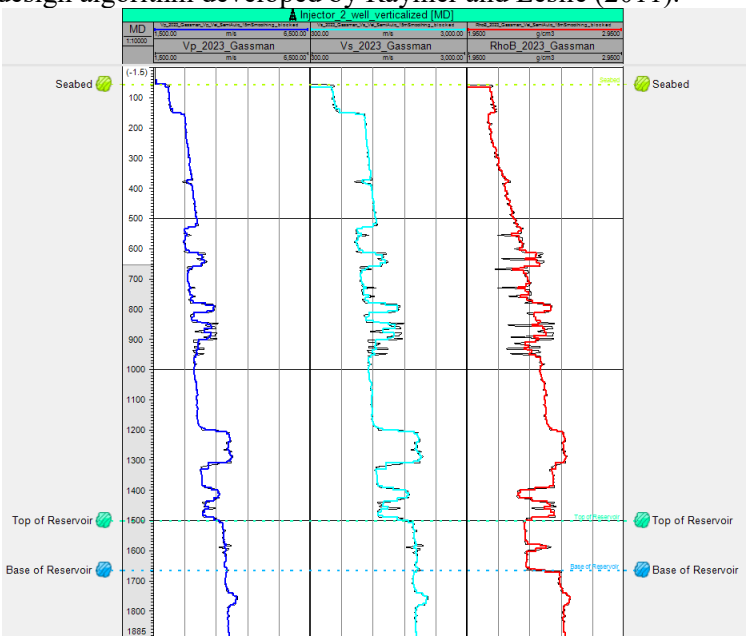


***Figure 1*** *Compressional (blue), shear (cyan) velocities, and density (red) logs, as well as the blocked model used for 1D network modelling.*

The process assumes a series of trial locations at regular intervals over a grid. Each trial location is evaluated numerically for a given set of sensor positions and arrival types (i.e., P-wave and/or S-wave)

at each station. This requires ray tracing through the velocity structure from the trial location to all the stations in the monitoring network to determine the partial derivatives at the trial location. This method also allows examining detectability limits by predicting signal-to-noise ratios (SNR) at receivers. The workflow considers the following:

- Sensor geometry—spatial distribution of sensors relative to potential event locations
- Sensor type—geophone, accelerometer, or DAS
- Velocity model including intrinsic attenuation (Qp and Qs)
- Source mechanism/radiation pattern
- Signal detection—signal amplitude (signal path) and noise (SNR)
- Measurement uncertainty—accuracy of time picking and hodogram angles

This study focuses on the sensor geometry and type for investigation. The tested microseismic detection networks are shown in Table 1.

| Array Type | Spatial Parameters | Number of Points |
|---|---|---|
| Ocean bottom seismometers | 327 $km^2$ | 16 (3 component geophones) |
| Downhole geophones | 300 m (700–1000 m depth) | 4 (3 component geophones) |
| S-DAS star array | 4 lines of 20 km length separated by 45°, injection well in the middle. Covering 314 $km^2$ | 257 points (DAS) |
| Downhole DAS | 1240 m (70–1310 m MD) | 63 (DAS) |
| S-DAS + Downhole DAS | Star array and downhole DAS together | 320 (DAS) |

***Table 1*** *Induced seismicity networks tested for a conceptual CCS site in Southern North Sea.*

The velocity model is built as described above, but the attenuation is not known in the area and is assumed to be $Q_p = Q_s = 100$. Similarly, assumptions around the source mechanism are beyond the scope of this project and a spherical radiation pattern is assumed. The typical range of microseismic event magnitudes (ML) considered in monitoring, measurement, and verification (MMV) studies is -3 to 2, and this study uses ML = 2 as the magnitude of events used to investigate the uncertainty of event location. The background noise is assumed to be $10^{-5}$ m/s for geophones, and $10^{-9}$ m/s for DAS, whilst the measurement uncertainty for time picking is 1 ms for P arrivals and 2 ms for S arrivals. For comparison, geophone hodogram uncertainty is 5° and not applicable to the DAS as it is a 1D measurement. The injection interval is 1500 m below the seabed, and the analysis area, where the various performance volumes such as detectability and uncertainty are computed, extends 600 m above and 400 m below this target zone, covering the primary seal, overburden, and underburden. The extent of the target area is 8 km x 8 km around the injection site.

**Results**

The results of network design for the ocean bottom seismometer (OBS)-type network are shown in Figure 2. In this scenario, the minimum detectable magnitude is defined as the ability to detect a microseismic event on at least one three-component OBS node. The immediate observation is that the detectability and uncertainty volumes exhibit bullseyes immediately below the sensors. This suggests that the proposed OBS-type network requires significantly more sensors to homogeneously cover the subsurface at and above the injection level (shown as depth slices in Figure 2). The minimum detectable ML is -1.5, and events in the $-1.5 < ML < -1$ range need to be within 1 km of each sensor at target level to be detected. For events with ML = 2, the maximum distance to be detected at target level is 2.5 km. However, the vertical uncertainty for events of ML = 2 is more than 100 m at 820 m offset from any OBS sensor (more than 200 m at 2 km offset). Horizontal uncertainty for an ML = 2 event is less than 100 m within 1.7 km of the sensor location. On the balance of these findings, events with $ML \leq 2$ can be detected and competently located within 1.7 km of the sensor at target level (1.5 km below seabed). These results are used as the baseline to compare to other networks.

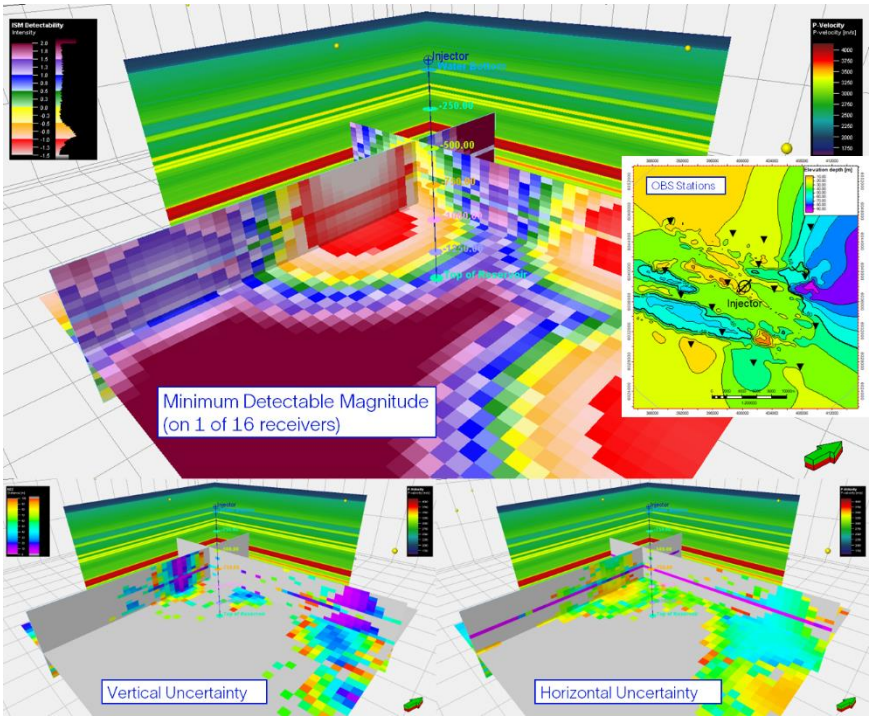


***Figure 2*** *Minimum detectable magnitude with OBS network of 16, randomly distributed sensors (top: insert shows map of OBS on seabed), vertical uncertainty (bottom left), and horizontal uncertainty (bottom right).*

Permanent downhole geophones have been used in the resource industry for over 20 years to monitor production as well as sequestration (Jones and Wason 2004). The most common long-life tool is deployed on tubing and has four sensor packages, separated by 100 m, containing four tetrahedrally arranged geophones. Based on the 1D model, and a range of possible microseismic event depths (constant offset from wellbore of 500 m), the best downhole location for the sensor network is 700–1000 m depth (Figure 3). This depth has the smallest detectable magnitudes with the least spread. This depth is chosen for the determination of the detectability and uncertainty volumes (Figure 4).

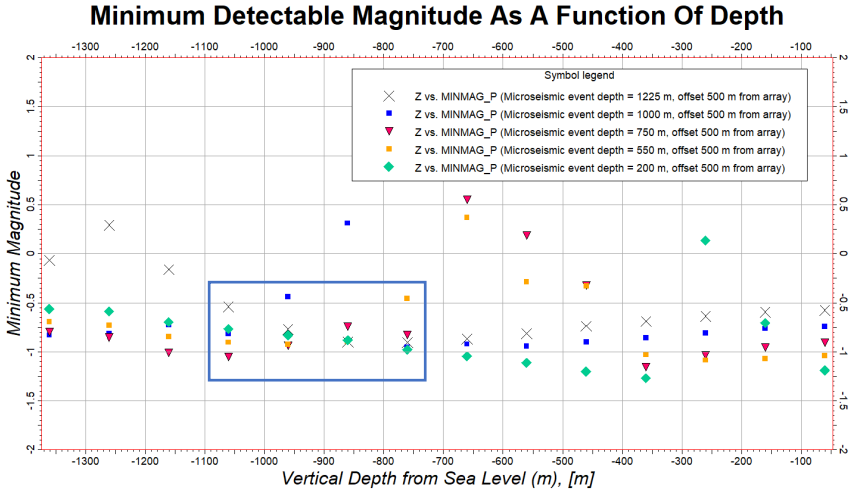


***Figure 3*** *Minimum detectable magnitude along the injector wellbore for microseismic events located 500 m away from the wellbore at depths of 1225, 1000, 750, 550, and 200 m. Optimum location shown in the blue box.*

In this scenario, the minimum detectable magnitude is defined as the ability to detect a microseismic event on at least one three-component geophone array. The performance of this network is improved in

terms of detectability of microseismic events, as it can record events in the -2 < ML ≤ 2 range with low positional uncertainty (<100 m) within 1.4 km at target level. For events with ML = 2, the maximum distance to be detected at target level is 2.5 km, similar to the OBS. The detectability is even better at shallower depths, across the receiver array. However, due to the singular location of such a network within the wellbore, the full field coverage is limited to the area around that wellbore.

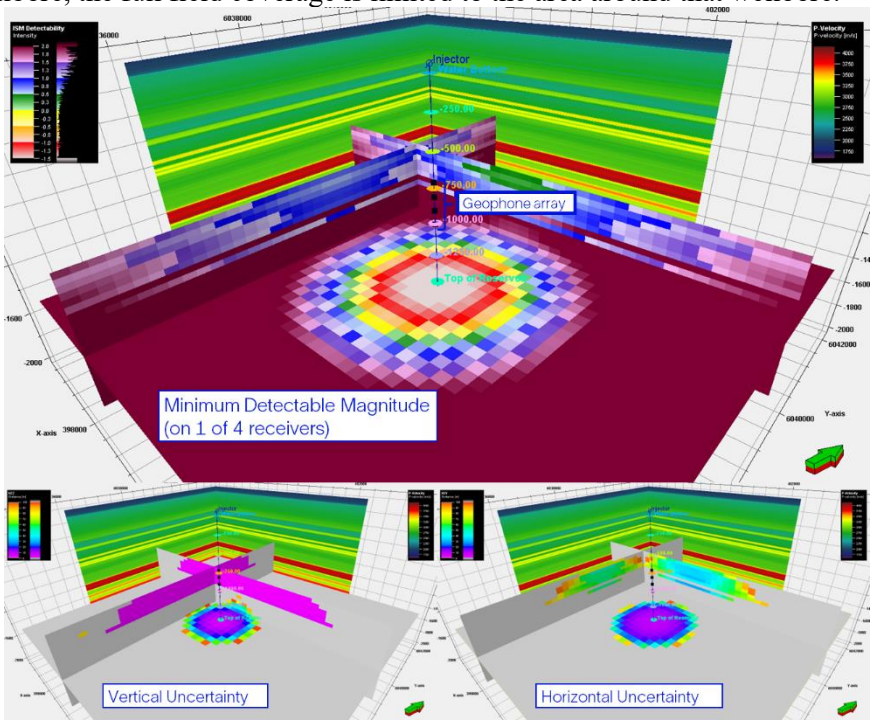


***Figure 4*** *Minimum detectable magnitude with 4-level geophone network (top), vertical uncertainty (bottom left,) and horizontal uncertainty (bottom right).*

DAS networks are an emerging technology for induced seismicity monitoring, and they have been successfully used for the acquisition of VSPs, both on retrievable and permanently installed fibres (Hartog et al. 2013; Frignet and Hartog 2014; Kimura and Galybin 2017). The coupling challenges associated with such networks are beyond the topic of this paper and could be overcome with some planning; hence, the coupling of fibre to the formation is assumed to be unimpacted by operational constraints, and the performance of such a network is shown in Figure 5.

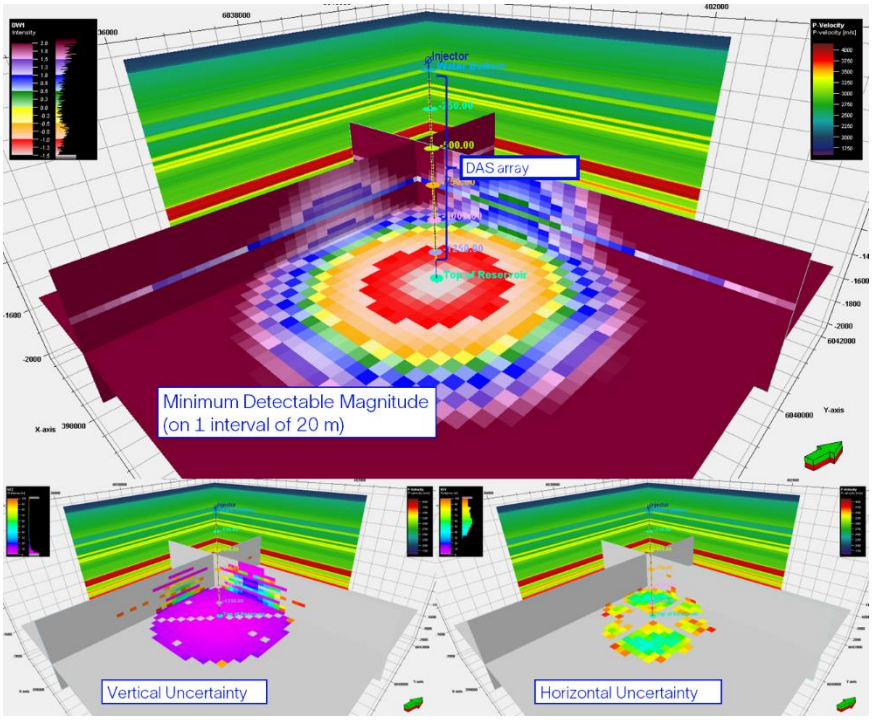


***Figure 5*** *Minimum detectable magnitude with an in-well DAS network (top), vertical uncertainty (bottom left), and horizontal uncertainty (bottom right).*

In this scenario, the minimum detectable magnitude is defined as the ability to detect a microseismic event on at least one 20 m interval downhole of the DAS measurement. The detectability of the DAS network is an improvement over the geophone and OBS networks, with the ability to record events in the $-2 < ML \leq 2$ range within 2.8 km of the injector. It should be noted that if the detection criterion is altered to the ability to detect on three 20 m intervals (for a fairer comparison to subsequent examples), the detectability for events is reduced to the $-1 < ML \leq 2$ range within 2.2 km of the injector. Also, the vertical uncertainty for an $ML = 2$ event is less than 100 m within a 2.2 km radius; however, the horizontal uncertainty is poor due to the axial nature of the DAS measurement. To overcome this limitation, either the instrumented wellbore needs to have a complex 3D profile or the DAS array needs to be supplemented by additional networks on the surface. S-DAS is one such type of network.

The performance of combined surface and downhole DAS networks is shown in Figure 6. Here, the minimum detectable magnitude is defined as the ability to detect a microseismic event on at least one 20 m interval downhole and at least one 300 m surface interval on two different lines. This condition allows for 3D event location in the subsurface but also means that the magnitude of events that can be detected is generally larger (Figure 6) than in the pure downhole DAS scenario (Figure 5). Such an arrangement allows for the detection of events in the $-0.8 < ML \leq 2$ range within 2.8 km of the wellbore. Nevertheless, the spatial uncertainties in locating an $ML = 2$ event are significantly smaller than with the use of only the downhole DAS. The use of S-DAS significantly extends the detectability of microseismic events away from the wellbore, especially close to the S-DAS lines. It is therefore prudent to investigate the performance of S-DAS on event detection on its own.

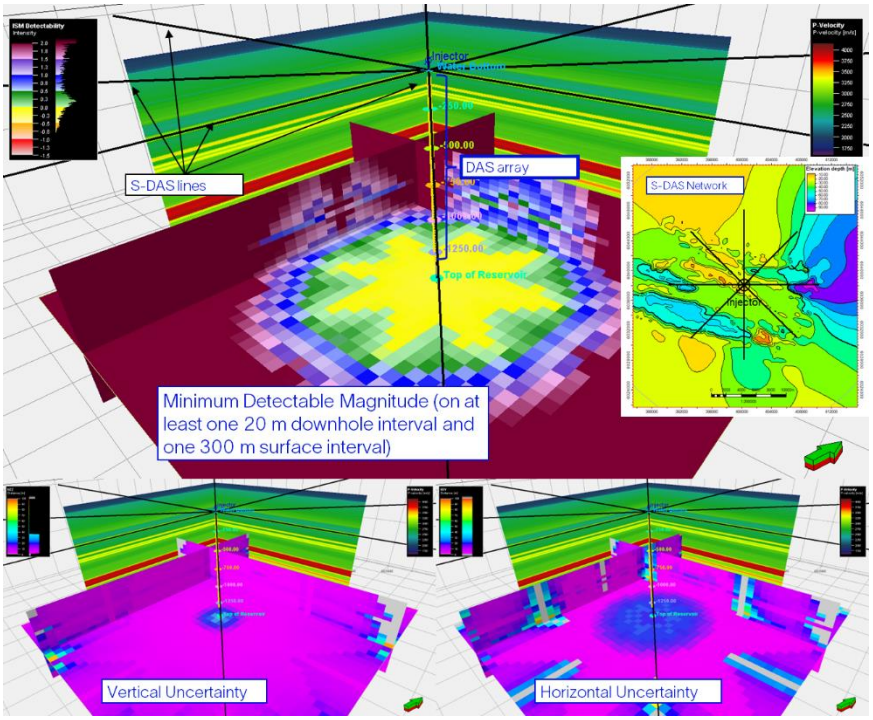


***Figure 6*** *Minimum detectable magnitude with a joint in-well and surface DAS network (top), vertical uncertainty (bottom left), and horizontal uncertainty (bottom right).*

S-DAS networks have recently been shown to be effective at monitoring time-lapse seismic response (Bachrach et al. 2023). The performance of the star-shaped S-DAS network is shown in Figure 7. Here, the minimum detectable magnitude is defined as the ability to detect a microseismic event on at least one 300 m surface interval on any three of the four lines. When comparing to the results of the joint downhole and surface DAS networks (Figure 6), the lack of the downhole component results in a decrease in sensitivity near the wellbore (-0.8 < ML). Nevertheless, the detectability of events with ML ≤ 2 is homogeneous within 2.3 km of the wellbore.

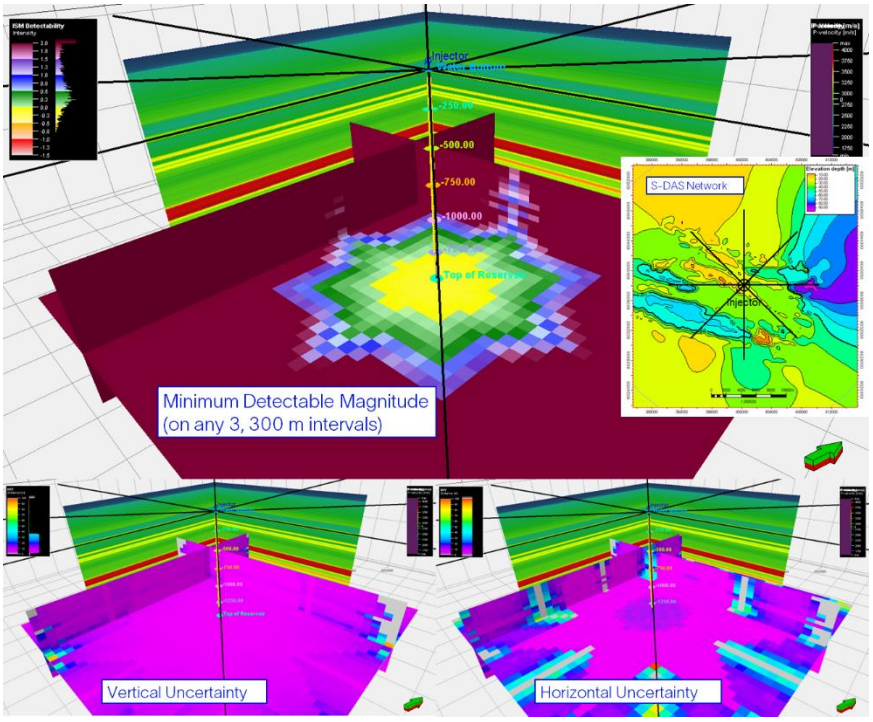


***Figure 7*** *Minimum detectable magnitude a surface DAS network (top), vertical uncertainty (bottom left), and horizontal uncertainty (bottom right).*

## Discussion

The five networks compared in this study can detect microseismic events below ML = 2 within at least 1.7 km of the injection wellbore. There is a general dependence on the number of receivers used for event detection, with an improvement in network sensitivity with an increasing number of receivers. This may seem trivial if one type of receiver is used; however, the comparison here is between three-component geophones and arrays of single-component DAS measurements, which are less sensitive and provide measurements only along the fibre, requiring at least three points (not in a single line) for 3D event location. There is also a dependence on the spatial extent of the receivers. The wellbore-only measurements can detect events within 1 km of the wellbore, with decreasing sensitivity as the wellbore offset increases. This is regardless of the type of network used. However, such networks have a low depth uncertainty compared to surface-deployed sensors, as shown in Figures 2–7. Conversely, horizontal uncertainty is low for downhole geophone arrays, whilst with a single array of downhole DAS, there is a 360° uncertainty on the event location. The performance is summarised in Table 2.

| Array Type | Detectability | 100 m Uncertainty Range (km) | 3D Location |
|---|---|---|---|
| Ocean bottom seismometers | -1.5< $M_L$ | 0.8 (1.7 for 200 m uncertainty) | YES |
| Downhole geophones | -2 < $M_L$ | 1.4 | YES |
| Downhole DAS | -1 < $M_L$ | 2.2 | NO |
| S-DAS + Downhole DAS | -0.8 < $M_L$ | 2.8 | YES |
| S-DAS star array | -0.8 < $M_L$ | 2.3 | YES |

***Table 2*** *Summary of induced seismic monitoring (ISM) array performance.*

The presence of surface measurements extends the spatial coverage significantly, regardless of the type of receiver. It is important to note that point receivers, such as the OBS, can detect microseismic events over a large area but require a large number to do so homogeneously, even with their improved sensitivity compared to the DAS measurement. In our example, one OBS sensor is needed per 9 $km^2$, but this is dependent on the velocity profile and attenuation. The major benefit of OBS is its relative ease of deployment. Deployment of S-DAS is more involved than the OBS but does not require access to downhole environments. S-DAS is shown to be as effective at detecting microseismic events as the OBS network, with homogeneous event detectability for events with -0.8 < ML within 2.3 km of the intersecting lines.

## Conclusions

Various induced seismicity monitoring technologies were investigated within the context of a hypothetical Southern North Sea CCS project. It was found that the combination of S-DAS and downhole DAS provides the best detectability and smallest event location uncertainty. The S-DAS network on its own also performs favorably, with a slight deterioration in terms of vertical event location uncertainty in comparison to a network augmented with downhole measurements. Nevertheless, other methodologies such as OBS and downhole geophones can provide adequate seismicity monitoring depending on local conditions. However, S-DAS networks do not require power and hence need significantly less interaction, making them an attractive and effective tool for induced seismicity monitoring.

**Acknowledgements** (Optional)
The authors thank the Net Zero Technology Centre (NZTC) for its funding in support of this project as part of their Open Innovation Program (Spark 2368). The authors also thank SLB Multiclient for the use of the horizons used in the static and dynamic modelling as well as the model parameters.

**References**

Bachrach, R., Branston, M., Harrington, S., Chapelle, M., Campbell, R., and Butt, J. [2023] An introduction to cost effective geophysical CCS monitoring using fiber optic cable deployed at the surface. 4th EAGE Global Energy Transition Conference & Exhibition, Paris 2023.

Branston, M., Bachrach, R., Chapelle, M., Harrington, S., Campbell, R., and Butt, J. [2024]. Adaptive monitoring of plume migration; evaluating the potential of surface DAS. EAGE Annual Conference and Exhibition, CCS Monitoring Workshop, Oslo, Norway, June 2024.

Frignet, B., and Hartog, A. [2014] Optical Vertical Seismic Profile on Wireline Cable. SPWLA 55th Annual Logging Symposium, May 18-22, 2014.

Harrington, S., Paydayesh, M., Danchenko, D., Fletcher, A., Ackers, M., Ward, C., and Pezzoli, M. [2023] Quantifying the predicted seismic response of $CO_2$ injection into a depleted gas reservoir. Energy Geoscience Conference, Aberdeen, May 16th.

Hartog, A.H., Kotov, O.I., and Liokumovich, L.B. [2013] The Optics of Distributed Vibration Sensing. Second EAGE Workshop on Permanent Reservoir Monitoring, Stavanger, Norway, Expanded Abstracts.

Jones, R., and Wason, W. [2004] PS3 – making the most of microseismic monitoring. Offshore Engineer, July 2004, pp 39-41.

Kimura, T., and Galybin, K. [2017] Borehole Seismic while Sampling Using FO Technology. 79th EAGE Conference & Exhibition, Paris, France, Expanded Abstracts.

Mizuno, T., Le Calvez, J. [2023] Quantitative Evaluation of DAS Passive Seismic Monitoring: Theory and Case Studies. 84th EAGE Annual Conference & Exhibition, Jun 2023, Volume 2023, p.1 - 5

Nakayama, S., Mouri, T., Podgornova, O., Armstrong, P., Lal Khaitan, M., Bettinelli, P., Le Calvez, J., Liang, L., and Zeroug, S. [2025] Elastic Anisotropic FWI for Multi-Well Walk-Away DAS-VSP Datasets in a CCUS Pilot Field Onshore Japan. IPTC-24966-EA, Feb 18-20, Kuala Lumpur.

Raymer, D.G., and Leslie, H.D. [2011] Microseismic Network Design - Estimating Event Detection. 73rd EAGE Conference & Exhibition, Vienna, May 2011.

Yamada, Y., Nakayama, S., Mouri, T., Lal Khaitan, M., Armstrong, P., and Podgornova, O. [2024] Imaging of multiwell and multifiber walkaway DAS-VSP datasets in a CCUS demonstration project onshore Japan. SEG Technical Program Expanded Abstracts, 503-507.